JOC The Journal of Organic Chemistry

Article

pubs.acs.org/joc

Stereoselective Gold(I) Domino Catalysis of Allylic Isomerization and Olefin Cyclopropanation: Mechanistic Studies

Sebastian Klimczyk,[†] Xueliang Huang,[‡] Hanspeter Kählig,[†] Luís F. Veiros,*[,§] and Nuno Maulide*[,†]

[†]Faculty of Chemistry, Institute of Organic Chemistry, University of Vienna, Währinger Strasse 38, 1090 Vienna, Austria

[‡]State Key Laboratory of Structural Chemistry, Fujian Institute of Research on the Structure of Matter, Chinese Academy of Sciences, 155 Yangqiao Road West, Fujian 350002, China

[§]Centro de Química Estrutural, Instituto Superior Técnico, Universidade de Lisboa, Av. Rovisco Pais 1, 1049-001 Lisbon, Portugal

Supporting Information

ABSTRACT: Gold(I) catalysis of olefin activation is still a rare feature in the repertoire of that metal. Mechanistic studies on the gold(I)-catalyzed cyclopropanation of allyl-substituted sulfonium ylides, including kinetic analysis as well as detailed computational studies, reveal that the reaction proceeds through activation of the alkene moiety. Furthermore, a novel competitive allylic isomerization pathway that interconverts "linear" and "branched" allylic isomers is uncovered. The subtle interplay of cyclopropanation and olefin isomerization results in an intriguing domino process where two independent catalytic transformations combine with near-perfect regio- and stereoselectivities.

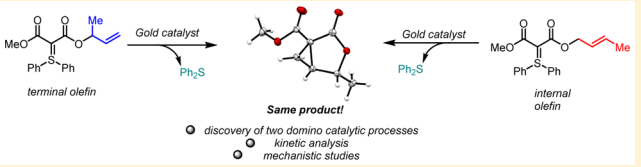

INTRODUCTION

The development and application of gold(I) catalysis in organic synthesis has witnessed an explosive growth over the last decades. The unique, almost unrivalled ability of various gold(I) species, ranging from simple salts to ornate organometallic complexes, to selective activate C−C multiple bonds under mild conditions is largely responsible for this.[1] A very large body of literature exists on the gold(I)-catalyzed activation of alkynes and allenes; comparatively, however, the activation of simple olefins for direct nucleophilic addition is by far less common.[2] Even in these rare instances, C−O and C−N bond-forming events appear to dominate the landscape;[3] gold(I) olefin activation leading to C−C nucleophilic bond formation is a rare class of transformations.[4]

In the course of our studies on gold(I)-catalyzed transformations of sulfur ylides, we discovered a catalytic cyclopropanation reaction (Scheme 1).[5,4f] Unusually, direct and indirect evidence suggested that this reaction proceeds by olefin activation rather than by metallocarbene formation. Herein, we present a thorough mechanistic study of the gold(I) stereoconvergent cyclopropanation of sulfonium ylides yielding reactivity insights that should prove useful for gold(I) catalysis of alkene activation in general. Additionally, we uncover an independent, facile gold(I)-catalyzed allylic isomerization that proceeds under similar conditions and ultimately results in a domino process of high efficiency and selectivity.

Scheme 1. Serendipitously Discovered Gold(I)-Catalyzed Cyclopropanation Reaction

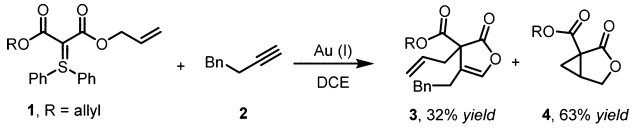

RESULTS AND DISCUSSION

We began our studies by carrying out kinetic measurements on the model substrate system **5** in the presence of Echavarren's catalyst **6**.[6] As shown in Figure 1, heating these two species at 80 °C in toluene delivered the cyclopropane **7** in a very clean reaction. This process reached 95% conversion after 6.5 h (Figure 1).

Reaction monitoring was also possible employing ^{1}H NMR spectroscopy (Figure 2), with a clear disappearance of the characteristic olefin resonances at δ = 4.6−6.0 ppm. Furthermore, the total concentration of **5** and **7** during the reaction was consistent with the concentration of **5** at t = 0, indicating that virtually no byproducts were formed. A logarithmic plot of [**5**] against time was characteristic of first-order behavior (Figure 3).

Encouraged by these observations, we performed further measurements at this temperature, obtaining consistent values for the rate constant (k_{av}(80 °C) = 8.27 × 10^{-3}). Carrying out kinetic measurements at different temperatures allowed the determination of the corresponding rate constants (Figure 4). This in turn enabled an estimation of the activation energy for this reaction of E_{act} = 21.11 kcal/mol.

Interested in the role of the catalyst in this reaction, we measured the rate constants of the reaction at various catalyst loadings. A plotting of the observed rate constants against the

Received: March 24, 2015
Published: May 27, 2015

DOI: 10.1021/acs.joc.5b00666
J. Org. Chem. 2015, 80, 5719−5729

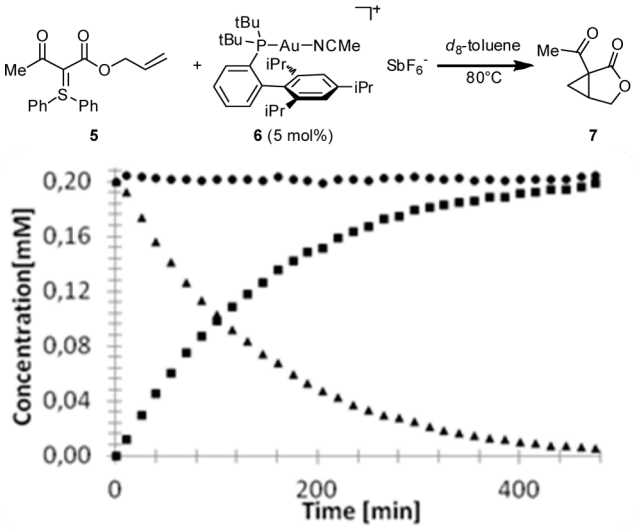

Figure 1. Gold(I)-catalyzed cyclopropanation of sulfonium ylide **5** where ▲= [**5**]; ■ = [7], and ● = [**5**] + [7], monitored by ^{1}H NMR spectroscopy.

catalyst loading (see the Supporting Information) afforded a straight line, documenting first-order behavior for the catalyst. Finally, we followed the reaction by ^{31}P NMR spectroscopy in order to assess the resting state of the catalyst during the process (Figure 5).

As shown, it would appear that the catalyst readily exchanges coordination to either the in situ liberated diphenyl sulfide (spectrum 2) or to the olefin (spectrum 3).[7]

The mechanism of cyclopropanation was further studied by DFT calculations.[8] The results obtained for the unsubstituted substrate **5** were the subject of a preliminary publication,[4f,9] and the corresponding profile is presented in Figure 6. The reaction pathway starts with a complex (**A**) where the substrate coordinates the metal fragment (M = $[Au(PPh_3)_3]^+$) by means of the C=C double bond in a η^2 mode. A rotation of the carbon backbone (**A** → **A′**) brings the ylide carbon and the inner carbon of the olefin into ideal proximity for the formation of the corresponding C–C bond. This bond is formed in the following step (**A′** → **B**), going through an early transition state, $\mathbf{TS_{A'B}}$, as shown by a very long distance (3.04 Å) and a negligible Wiberg index,[10] WI = 0.01.

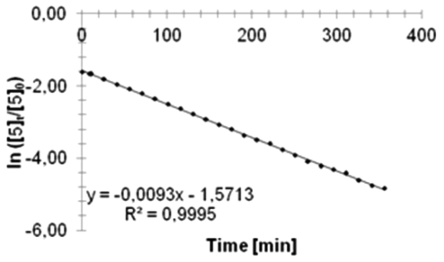

Figure 3. Representative plot of $\ln([\mathbf{5}]_t/[\mathbf{5}]_0)$ against the reaction time (min) for the conversion of **5** showing first-order dependence in **5**.

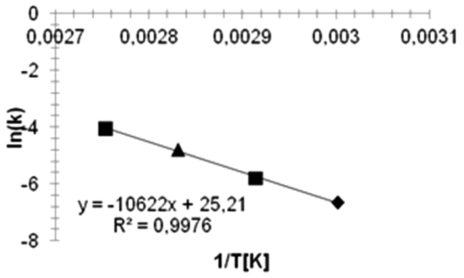

Figure 4. Plot of $\ln(k)$ against $1/T$ (K).

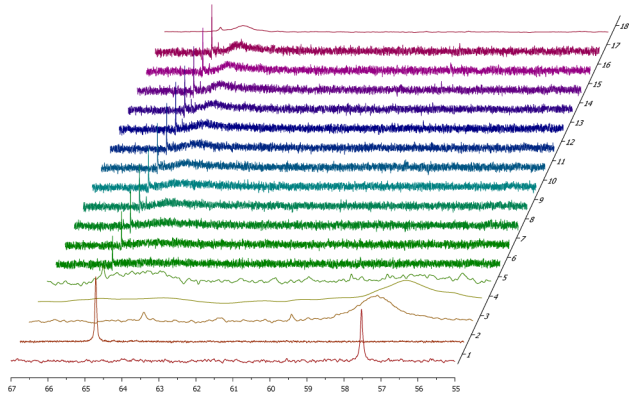

Figure 5. ^{31}P kinetics of the gold(I)-catalyzed cyclopropanation, spectra 4–18. Free catalyst **6** (spectrum 1), **6** + diphenyl sulfide (spectrum 2), and **6** + allyl acetate (spectrum 3).

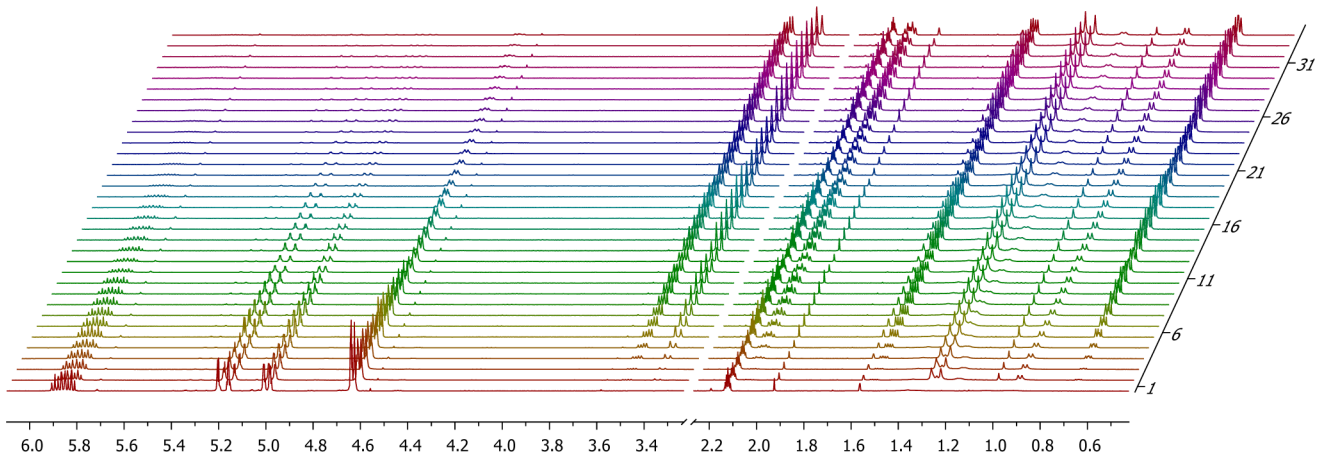

Figure 2. Enlargement of the allylic and aliphatic regions of the 400 MHz ^{1}H NMR spectra of the conversion of **5** to **7**. The aromatic region and the area between 2.2 and 3.3 ppm were omitted for clarity.

DOI: 10.1021/acs.joc.5b00666
J. Org. Chem. 2015, 80, 5719–5729

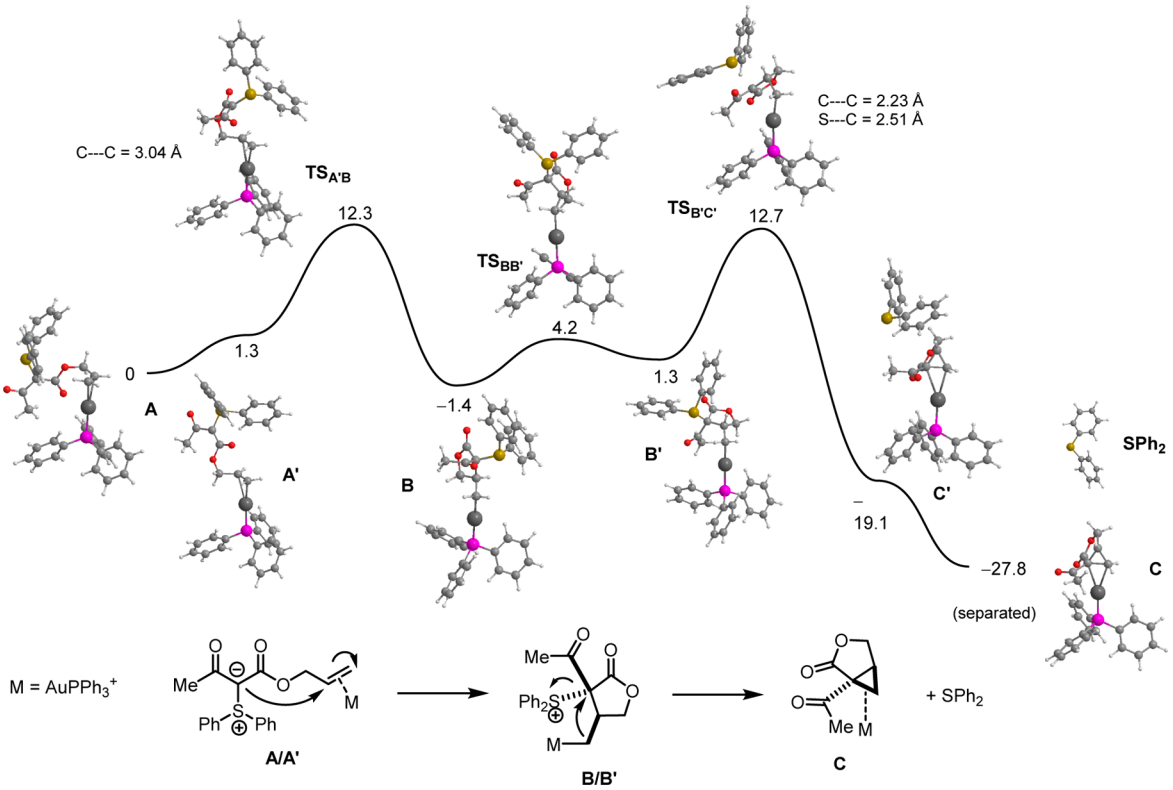

Figure 6. Free energy profile (PBE0) for cyclopropanation of the unsubstituted substrate. The minima and the transition states were optimized, and the structures obtained are presented with the more relevant bond distances in each step. Free energy values (kcal/mol) are referred to the initial intermediate (**A**).

Intermediate **B** corresponds to a 5-membered lactone carrying a gold−alkyl complex appended to the lactone β-carbon. The mechanism proceeds with a further conformational change (**B** → **B′**), by which the original ylidic carbon atom and the carbon bound to the metal center are brought to the right conformation for the establishment of the final C−C bond and, thus, cyclopropanation and loss of SPh_2 in the final step. Formation of the cyclopropane ring, from **B′** to **C′** occurs via transition state $\mathbf{TS_{B'C'}}$ where cleavage of the C−S bond is well advanced (d = 2.51 Å, WI = 0.34), whereas the new C−C bond is only incipient (d = 2.23 Å, WI = 0.23). The final product coordinates the metal moiety weakly in a σ-complex using the newly formed C−C bond of the cyclopropane in **C′** and **C**.[11a]

The mechanism depicted in Figure 6 entails two consecutive C−C bond-forming events: the first leads to the lactone ring in intermediates **B** and **B′** while the second corresponds to the formation of the cyclopropane ring in **C′** and **C**, and both present similar energy barriers (within 0.4 kcal/mol). The first C−C bond results from a formal nucleophilic attack of the ylidic carbon to the internal carbon of the activated C═C double bond. This is indicated by the respective atomic charges (NPA, see the Computational Details in the Supporting Information) calculated for intermediate **A′**, which clearly show a more electron-rich ylide carbon with a charge of C = −0.60, compared with the olefin carbon atom with C = −0.17. This is in agreement with the known reactivity of sulfur ylides. The nature of the second C−C bond formation event, effectively resulting in cyclopropanation, is perhaps more surprising. In fact, the atomic charges calculated for the relevant C atoms in intermediate **B′** present a more electron-rich coordinated carbon, C_{Au} (C = −0.93), when compared with the carbon carrying the Ph_2S moiety (C = −0.37). This suggests a nucleophilic attack from the bound metal−alkyl in a reactivity pattern similar to that of a typical organometallic C-nucleophile.[12] Frontier orbital analysis of intermediate **B′** (Figure 7) further confirms this assumption.

The HOMO of **B′** is a Au−C σ orbital with a significant (23%) contribution on the coordinated carbon, while the LUMO represents a C−S σ^* interaction with 12% of its electron density on the ylide C atom. This corroborates a cyclopropanation step occurring with electron transfer from the

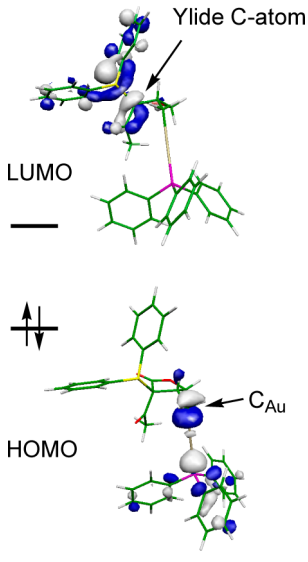

Figure 7. Frontier orbitals of intermediate **B′**.

DOI: 10.1021/acs.joc.5b00666
J. Org. Chem. 2015, 80, 5719−5729

coordinated C atom to the originally ylidic carbon, with consequent breaking of the C−S bond and loss of the leaving group. It is important to note that the reaction intermediate **B**/**B′** bears two stereogenic centers (see Figure 7). Therefore, four different stereoisomers corresponding to two pairs of enantiomers are possible. In one pair (**B′**), the carbon bound to gold (C_{Au}) and the SPh_2 group are *trans* to each other; in the opposite diastereomer, intermediate **D**, C_{Au} and the SPh_2 group occupy the same face of the lactone ring (Figure 8).

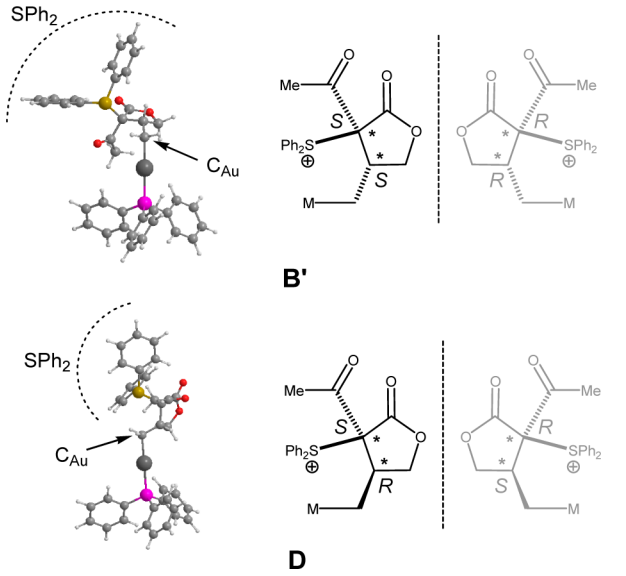

Figure 8. Diastereoisomeric intermediates **B′** and **D**.

Naturally, the geometrical constraints of the cyclopropane ring imply that the final product will be the same regardless of the stereochemistry of the intermediate. Nevertheless, different energy profiles should result for each case, and in the case of substrates with substituents (cf. Figure S14) the selectivity of the reaction will depend on the stereochemical features of the intermediate. Consequently, we also addressed the mechanism of cyclopropanation via intermediate **D**, and the profile obtained is presented as Supporting Information (cf. Figure S12). The main characteristics of the mechanism remain the same as in the path depicted in Figure 6 and discussed above. Thus, there are two consecutive C−C bond-forming events. Both energy barriers are higher than the ones calculated for the previous mechanism, via **B**/**B′**, being 19.9 and 25.4 kcal/mol for the two steps, respectively. Consequently, two main differences between these pathways emerge: (1) the mechanism proceeding via **B**/**B′** is more favorable than the one that includes intermediate **D** and (2) instead of two equally difficult steps, as observed in the first path, the second step (cyclopropanation) becomes clearly rate determining in the second mechanism. A closer observation of the transition states for the cyclopropanation step in both mechanisms explains those differences (Figure 9). While for $TS_{B'C'}$ formation of the C−C bond and loss of the SPh_2 leaving group occur in nearly antiperiplanar fashion, in the case of $TS_{DE'}$ those two processes take place on the same face of the lactone ring, the latter resulting in a significantly higher barrier.

Use of Substituted Allyl Moieties. If substituted allyl moieties are employed, interesting observations can be made. In case of substitution at the allylic position (Scheme 2), the corresponding cyclopropanation products could be isolated in good to excellent yields and in excellent stereoselectivities (typically >12:1).

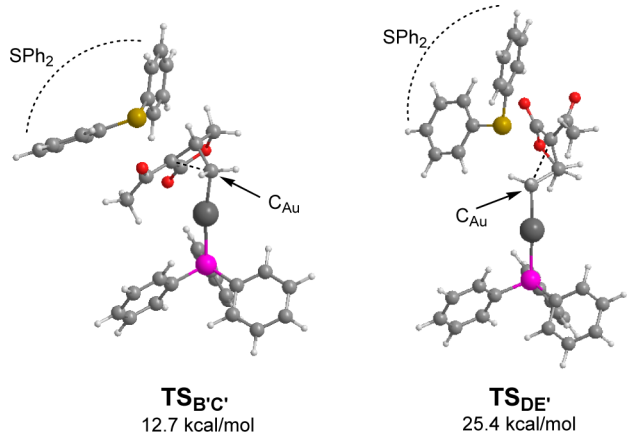

Figure 9. Transition states for the cyclopropanation step of the mechanism involving the two diastereomeric lactone intermediates, **B′** (left) and **D** (right). Free energy values (kcal/mol) relative to **A** are presented.

Scheme 2. Gold-Catalyzed Cyclopropanation of Substituted (Allyloxy)Sulfonium Ylides

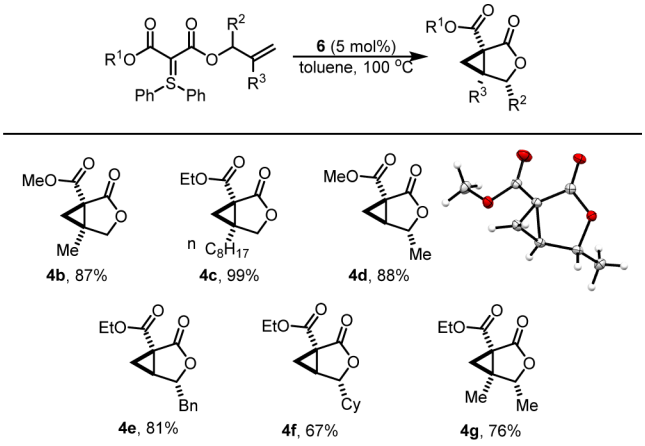

Unexpectedly, we found that the use of terminally substituted olefins such as **1h** in this cyclopropanation reaction leads to formation of **4d**, the same product (with similarly high diastereoselectivity) we had previously observed when employing branched allyl moieties. This was the case regardless of the *E*/*Z* geometric purity of the starting materials (Scheme 3b).

Scheme 3. Apparent Allylic Rearrangement upon Attempted Cyclopropanation of Terminally Substituted Olefins

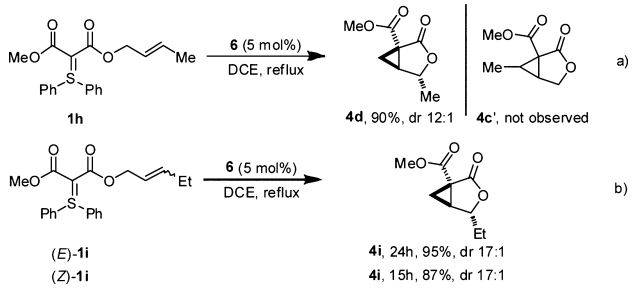

DOI: 10.1021/acs.joc.5b00666
J. Org. Chem. 2015, 80, 5719−5729

With this finding in mind, we were interested in cyclizing the enantiopure ylide (*R*)-**1j** (ee >99%), hoping to thus obtain the corresponding enantiopure cyclopropane **4j**. Surprisingly, however, the resulting product, while still essentially a single diastereomeric substance, was nearly devoid of optical activity (Scheme 4a). As such a result must imply transient loss of tetrahedral character at C1′, we prepared the deuterated substrate **1k** and submitted it to the cyclopropanation reaction conditions (Scheme 4b). In the resulting cyclopropane product, 12% of deuterium scrambling could be unambiguously detected by NMR analysis of the crude mixture.[13]

Scheme 4. (a) Cyclopropanation of an Enantiopure Sulfonium Ylide. (b) Isotope-Labeling Experiment

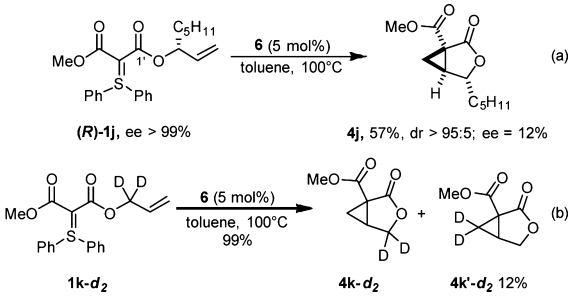

This interesting result suggested that not only an allylic rearrangement occurs during the reaction with gold(I) catalyst **6**, but also that the interconversion between allylic isomers of the substrate competes with the cyclopropanation reaction. In order to gain further understanding of this phenomenon, the mechanisms of interconversion between substrates were studied by DFT and compared with those calculated for the formation of each one of the four possible isomers of the product. The first process addressed is the isomerization between branched and linear substrates, for which the profile presented in Figure 10 was obtained.

The initial species in the reaction profile, **F**, is an η^2 complex where the branched substrate binds to the metal atom through the C═C double bond, similarly to what happens in complex **A** for the unsubstituted substrate (Figure 6). From **F**, a rotation around the COO−C bond brings the O atom of the ester carbonyl group close to the terminal carbon of the olefin, ultimately resulting in intermediate **G**. This corresponds to a cyclic 6-membered acetal carrying a metal−alkyl fragment. In the corresponding transition state, $\mathbf{TS_{FG}}$, the new C−O bond is still far from established with a long distance (2.13 Å) indicating a weak interaction (WI = 0.22), while the metal center is clearly sliding toward the internal olefinic carbon, with differentiated Au−C distances of 2.58 and 2.17 Å (compared with 2.27 and 2.32 Å in **F**). The second step (**G** → **H**) is equivalent to first one. Here, the other C−O bond of the acetal breaks, regenerating the carbonyl group but now bearing a linear allylic moiety. The overall process depicted in Figure 10 corresponds to a facile reaction with a barrier of 14.6 kcal/mol associated with the first step.

To complete the isomerization study, one has to consider the interconversion between the two isomers involved in the previous mechanism (branched and linear *E*) with the third stereoisomer, i.e., the linear *Z* species. Since a direct interconversion between the *E* and *Z* isomers of the linear substrate would involve a prohibitive rotation around a C═C double bond, the actual change occurs via the branched isomer. However, the shift of the ester group from one olefin C atom to the other, through a cyclic acetal intermediate similar to **G** (Figure 10), must take place with the appropriate conformation of the carbon chain in order to yield the *Z* isomer of the linear substrate.

In the acetal intermediate that leads to the linear *E* isomer (**G**), the metal center and the methyl group have a *trans* orientation along the six-membered ring (see Scheme 5a),

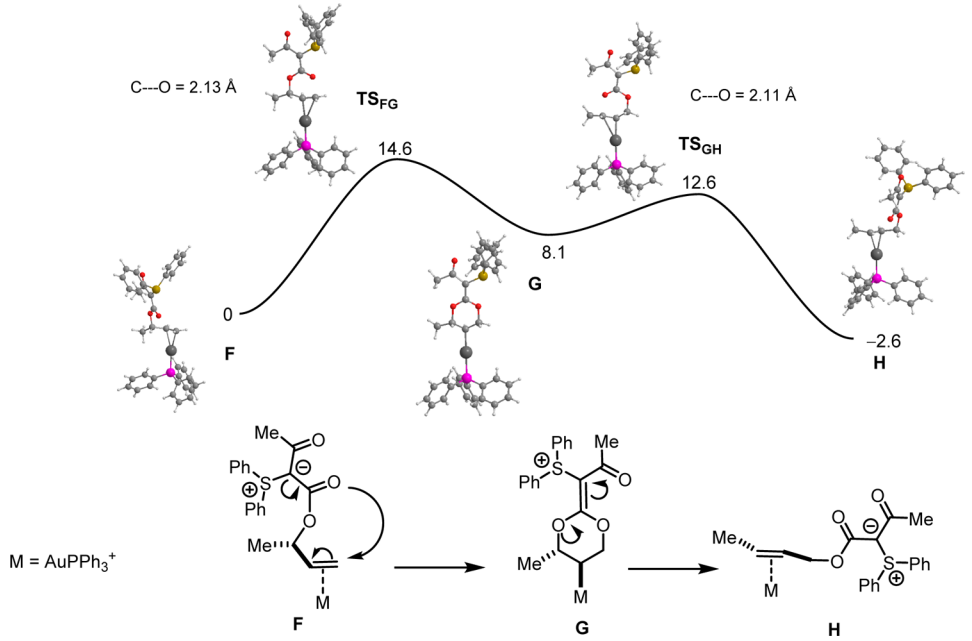

Figure 10. Free energy profile (PBE0) for interchange between the branched substrate and its *E* linear isomer. The minima and the transition states were optimized, and the structures obtained are presented with the more relevant bond distances in each step. Free energy values (kcal/mol) are referred to the initial intermediate (**F**).

DOI: 10.1021/acs.joc.5b00666
J. Org. Chem. 2015, 80, 5719−5729

Scheme 5. Relevant Conformations of the Intermediates in the *E*−*Z* Isomerization Process

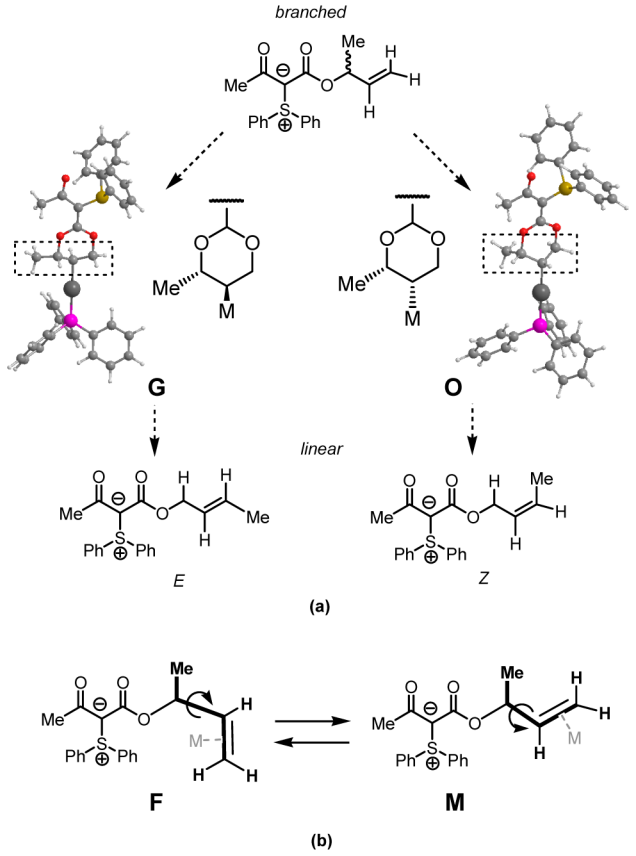

while in the equivalent intermediate that yields the *Z* isomer (**O**) those two fragments are *cis* to each other. This relates to two different conformations of the Me−C−CH=CH$_2$ chain in the initial η^2 complex of the branched substrate that interchange through a rotation around the allylic C−C bond. One conformer (Scheme 5b, left) will lead to the *E* linear substrate (cf. **F** in Figure 10), while the other (Scheme 5b, right) will produce the *Z* linear substrate, corresponding to intermediate **M** in the profile depicted in Figure 11. The energy profile calculated for the interconversion between the two relevant conformers of the η^2 complex of the branched substrate is provided in the Supporting Information as Figure S15 and attests to a facile process with a maximum barrier of 7.5 kcal/mol.

The energy profile calculated for the branched-to-linear *Z* isomerization is depicted in Figure 11. The first step in the mechanism depicted in Figure 11 corresponds to rotation around the COO−C bond bringing the ester carbonyl oxygen into proximity of the internal olefin carbon, converting **M** into the intermediate **N**. The transition state, **TS$_{MN}$**, is reached when the carbonyl group passes by the methyl substituent and, thus, at a rather long O−C distance (3.98 Å). Intermediate **N** is a five-membered cyclic acetal that coordinates the metal as an alkyl ligand. In the following step, from **N** to **O**, there is a simultaneous 1,2-shift of the O−C and of the Au−C bonds such that the metal and the O atom exchange carbon atoms. The result is an expansion of the acetal from a 5-membered ring in **N** to a 6-membered ring in **O**. In the corresponding transition state, **TS$_{NO}$**, formation of the new O−C bond (2.14 Å, WI = 0.21) is well advanced and the previous one is practically cleaved (2.70 Å, WI = 0.04), while the Au atom is much closer to the inner olefin C atom (2.17 Å) than to the outer one (2.58 Å). In the final step of the mechanism, the acetal ring is opened through the breaking of one O−C bond, yielding the η^2 complex of the *Z* linear isomer of the substrate in **P**. This step is equivalent to the one that leads to the coordinated *E* linear isomer (via **TS$_{GH}$**), discussed above. The highest barrier is associated with the ring-expansion step, going through **TS$_{NO}$**, and its value (16.3 kcal/mol, relative to **F**) is only 1.7 kcal/mol higher than the one obtained for the branched-linear *E* isomerization path (Figure 10). In summary, the entire isomerization process interconverting the branched and linear *E* and *Z* allylic isomers is represented by the combination of the energy profiles in Figures 10 and 11 and Figure S15 (Supporting Information) and, thus, requires the overcoming of a maximum energy barrier of 16.3 kcal/mol (corresponding to **TS$_{NO}$**). This indicates a process that should occur easily under the experimental conditions of the reaction.

Further experimental evidence for this facile isomerization (Figure 12) was readily obtained by exposure of the simple but-2-enyl methylmalonate **8** (not carrying a sulfur ylide moiety) to the action of gold catalyst **6** in deuterated chloroform.[14] Comparison of the NMR spectra of pure "branched" isomer **9** with that of the reaction mixture unambiguously reveals the presence of the "linear" isomer in both (*E*) and (*Z*) forms, thus corroborating the computational data. Further, it confirms this isomerization process as being independent of the sulfur ylide appendage.

Having established and understood the grounds for isomerization, we now sought to understand the remarkable stereo- and regioconvergence of this transformation that enables the formation of a single product from an interconverting mixture of isomers (and regardless of the substrate isomer employed). The DFT profile illustrated in Figure 13 represents the mechanism of formation of product **R**, i.e., the major regio- and stereoisomer of the cyclopropane product that is experimentally obtained. The path calculated for the formation of **R** from the branched substrate is entirely equivalent to the mechanism calculated for the unsubstituted substrate, discussed above (Figure 6).

Thus, it comprises two consecutive steps with C−C bond formations in each. After a rearrangement of the carbon chain of the substrate, from **F** to **F′**, there is formation of the lactone ring in intermediate **Q**. In all mechanisms calculated for the cyclopropanation of substituted substrates (R = Me) the lactone intermediate forms as the stereoisomer with the coordinated C atom (C_{Au}) and the SPh_2 is *trans* relative positions, since this was shown to be the most favorable intermediate from the stereochemical point of view (see Figure 9 and the corresponding discussion above). In transition state **TS$_{F'Q}$** the new C−C bond is only incipient as shown by a very large distance (2.63 Å) and a negligible Wiberg index (WI = 0.09). The final step of the mechanism corresponds to the formation of the C_3 ring and loss of SPh_2, from **Q** to **R′**. In the transition state, **TS$_{QR'}$**, the relevant bond lengths (d_{C-C} = 2.19 Å, d_{C-S} = 2.50 Å) indicate that both C−S bond breaking and C−C bond formation are halfway through once the transition state is reached. The highest barrier in the profile depicted in Figure 12 corresponds to the formation of the lactone ring (**TS$_{F'Q}$**), being 16.4 kcal/mol.

The mechanisms that lead to the formation of each one of the other three isomers of the cyclopropane product, **T**, **V**, and **Y**, were also calculated, and the corresponding energy profiles

DOI: 10.1021/acs.joc.5b00666
J. Org. Chem. 2015, 80, 5719−5729

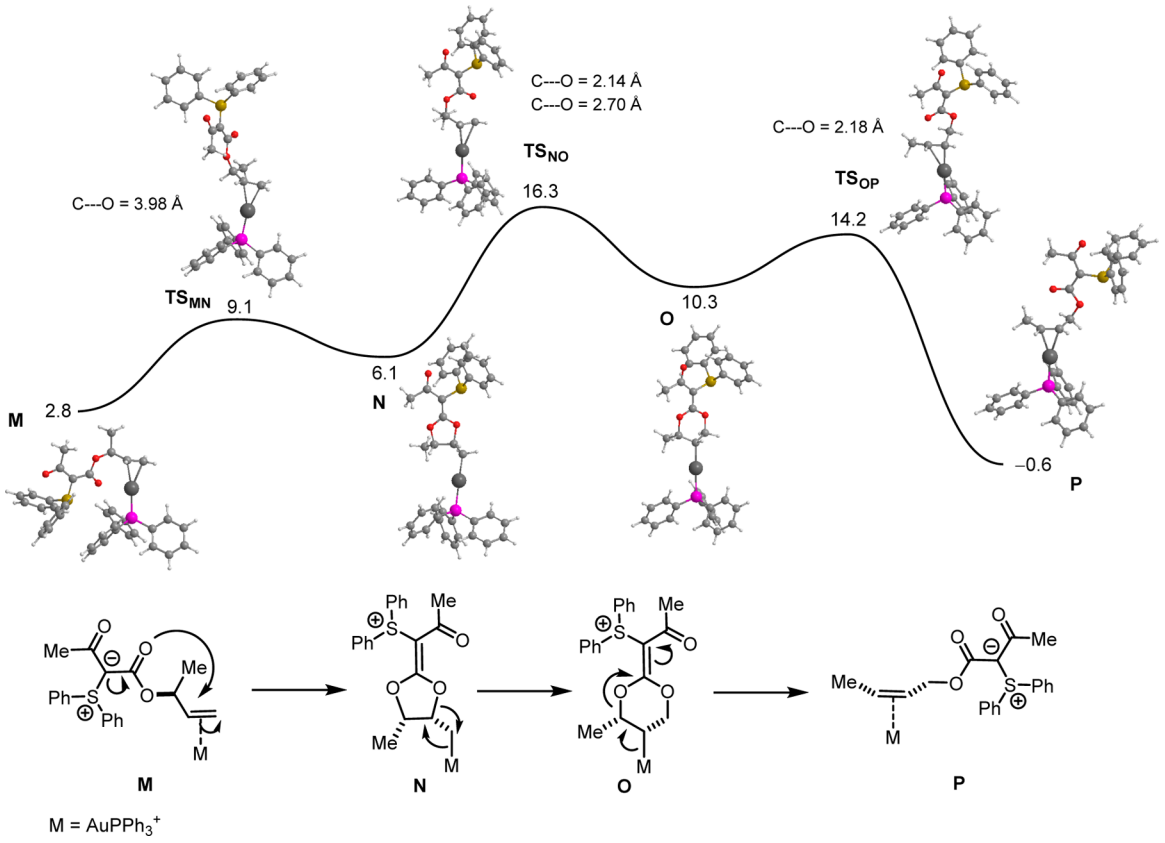

Figure 11. Free energy profile (PBE0) for interchange between the branched substrate and its *Z* linear isomer. The minima and the transition states were optimized and the structures obtained are presented with the more relevant bond distances, in each step. Free energy values (kcal/mol) are referred to intermediate **F**.

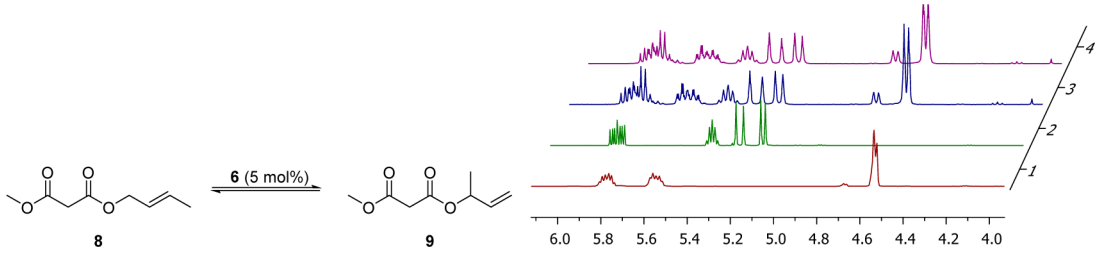

Figure 12. ^{1}H NMR spectra of (*E*)-**8** (spectrum 1), pure **9** (spectrum 2), mixtures of pure (*E*)-**8** + 5 mol % of gold complex **6** after 2 h (spectrum 3) and after 7 h (spectrum 4; here, a mixture of **9** and (*E*)- and (*Z*)-**8** is visible).

are presented in the Supporting Information (Figures S16, S17, and S18). The main characteristics of those paths are similar to the one obtained for product **R**, discussed above and, thus, require no further discussion. However, the energy barriers obtained for those mechanisms (19.0−22.2 kcal/mol) are all higher than the ones calculated for the formation of **R**, indicating that this is the most favorable of all four cyclopropanation mechanisms.

Thus, on one hand, it emerges that cyclopropanation is always preferred from the "branched" allyl isomer rather than from the "linear" analogue (i.e., **T**/**R** preferred over **Y**/**V**, Figure S14, Supporting Information). This is reflected in higher energy barriers for the second mechanistic step, namely the formation of the three-membered ring. The energy barriers practically double from one type of substrate to the other, going from 13.5 kcal/mol ($\mathbf{TS}_{QR'}$) and 12.0 kcal/mol ($\mathbf{TS}_{ST'}$) to 18.8 and 22.2 kcal/mol in $\mathbf{TS}_{UV'}$ and $\mathbf{TS}_{WY'}$, respectively. In fact, for the "linear" substrates the second step of each mechanism has an energy barrier either similar to (Figure S17) or even higher than the first step, becoming rate determining in the formation of product **Y** from the *Z* isomer of the "linear" substrate (Figure S18). Again, it is the stereochemical disposition of the various groups around the C−C bond that is being formed that dictates the differences observed (Figure S20). Here, the steric hindrance caused by the presence of a methyl substituent in the terminal C_{Au} atom hampers the formation of the corresponding C−C bond, destabilizing the transition state and raising the barrier.

The two cyclopropanation mechanisms for the branched substrate, leading to the two possible different diastereoisomers, are represented in the profiles of Figure 13 (*cis* product **R**) and Figure S16 (*trans* product **T**). The major difference between the two profiles is the first step (i.e., formation of the lactone intermediate). Here, the stereochemical repulsion between the methyl and the acyl groups in the corresponding transition

DOI: 10.1021/acs.joc.5b00666
J. Org. Chem. 2015, 80, 5719−5729

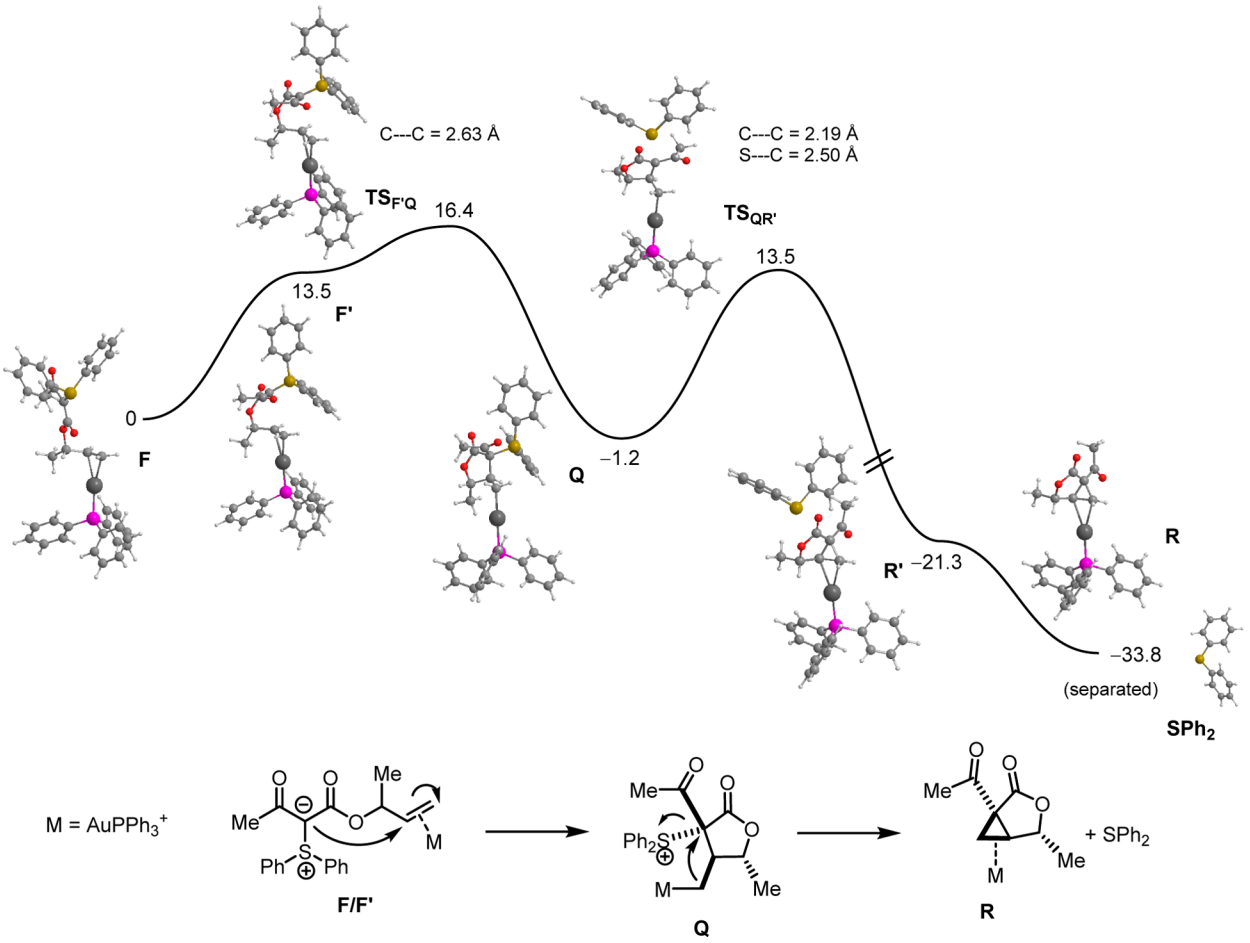

Figure 13. Free energy profile (PBE0) for cyclopropanation of the branched substrate yielding product **R**. The minima and the transition states were optimized, and the structures obtained are presented with the more relevant bond distances in each step. Free energy values (kcal/mol) are referred to the initial intermediate (**F**).

states (see the Supporting Information, Figure S19) results in a difference of 2.6 kcal/mol in the corresponding barriers.

Validation of the Computational Predictions. The mechanistic studies described above afford two main conclusions. First, the isomerization process has an overall energy barrier similar (**TS$_{NO}$**, Figure 12) to the one presented by the cyclopropanation reaction that forms product **R** (**TS$_{F'Q}$**, Figure 13). In fact, the values are within 0.1 kcal/mol and can be considered equal at the level of theory employed. The second equally important result is that all cyclopropanation paths that lead to the formation of the other three isomers of the product (**T**, **V**, and **Y**) have higher energy barriers and, thus, are less favorable than both substrate isomerization and formation of **R**. This means that all substrate isomers interconvert faster than any cyclopropanation reaction occurs, except the one that produces **R** thus explaining the high regio- and stereoselectivity of the process. The ability of gold to not only catalyze both processes in what is effectively a domino allylic isomerization/cyclopropanation, but also to do so with such high selectivity is remarkable.

To validate these conclusions, we prepared several "linear"-allyl-containing sulfur ylides and submitted them to the cyclopropanation conditions. As shown in Schemes 3 and 6, all linear substrates yield the corresponding "branched" cyclopropanes, with substituents in the 4-position, in very good to excellent diastereoselectivities. As predicted by DFT,

Scheme 6. Cyclopropanations of "Branched" Substrates

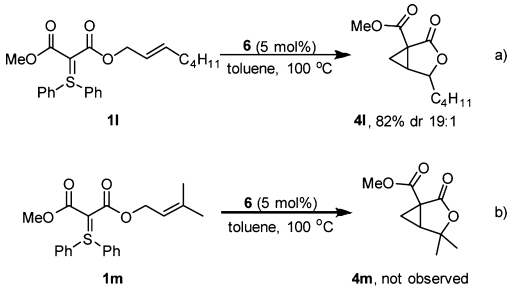

using either the *E*- or *Z*-olefin isomer of the substrate led to the same product isomer in virtually identical yields and diastereoselectivities (Schemes 3b and 6a). Isomerization under these conditions appears to be limited to disubstituted olefins, as use of a prenylated substrate blocks the reaction and only starting material could be recovered (Scheme 6b).

Two additional experiments shed more light on the peculiarities of these coupled processes (Scheme 7a). The failure of double-substituted substrate **1o** to undergo any reaction (substrate recovered unchanged) implies that cyclopropanation of a "linear" allyl substrate has a prohibitively high barrier under these conditions. It is worthy of note that the allylic rearrangement of **1o** is a degenerate process.

DOI: 10.1021/acs.joc.5b00666
J. Org. Chem. 2015, 80, 5719−5729

Scheme 7. (a) Blocking the Cyclopropanation with 1,3 Disubstitution (b) and Using the Amide Bond in 10 To Force Cyclopropanation of a "Branched" Substrate

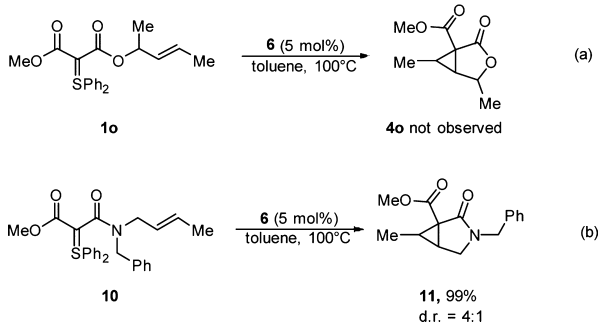

In contrast to this, the crotyl amide **10** underwent cyclopropanation and afforded the 6-methyl cyclopropanation product **11** (as determined by 2D-NMR analysis) in quantitative yield and a dr of 4:1 (Scheme 7b). This is the only instance where we have observed cyclopropanation of an internal olefin. It is reasonable to assume that the hypothetical isomerization process (converting the amide in **10** to an O-allylated imidate) becomes energetically much less favorable (or even prohibitive).[15] In addition, the conformational rigidity of amides may also contribute to a lowering of the energy barrier for cyclopropanation. The conjunction of these two factors presumably brings the hurdle for cyclopropanation of an internal olefin to a surmountable value in **10**.

CONCLUSIONS

In conclusion, we have presented a detailed study on a gold-catalyzed olefin cyclopropanation that unusually proceeds by a two-step mechanism critically hinging on olefin activation by the metal catalyst. The mechanistic consequences of that include not only a very high specificity of the individual steps but also the emergence of a parallel, rapid (under the reaction conditions), gold-catalyzed allylic isomerization process. The latter is independent of the cyclopropanation transform; when coupled to cyclopropanation, it results in very high regio- and stereoselectivity. That the same metal promotes two independent transformations which can function in tandem with such high selectivity is testimony to the versatility of gold in catalysis.

EXPERIMENTAL SECTION

Unless otherwise indicated, all glassware was flame-dried before use, and all reactions were performed under an atmosphere of Argon. All solvents were distilled from appropriate drying agents prior to use. All reagents were used as received from commercial suppliers unless otherwise stated. HRMS measurements were carried out with an ESI QqTOF mass analyzer. All the ylides were prepared according to the procedures reported by our group.[16] Compounds **4b−g** were prepared following a procedure reported by our group.[4f]

General Procedure for the Preparation of Sulfonium Ylides. To a solution of Martin's sulfurane (336 mg, 0.5 mmol) in CH_2Cl_2 was added a solution of 1,3-dicarbonyl compound (0.5 mmol). After the mixture was stirred at room temperature for 2 h, all volatiles were removed *in vacuo*, and the crude mixture was purified by column chromatography over silica.

*(R)-Methyl Octen-3-yl 2-(Diphenylsulfuranylidene)malonate (**1j**).* The compound was prepared following the general procedure. Purification by column chromatography over silica (*n*-pentane/ethyl acetate 1/1) afforded the title compound as colorless oil (206 mg, 0.5 mmol, 99%). R_f = 0.46. ^{1}H NMR (300 MHz, $CDCl_3$): δ = 7.67−7.57 (m, 4H), 7.55−7.39 (m, 6H), 5.76−5.59 (m, 1H), 5.32−5.21 (m, 1H), 5.17 (dt, J = 17.2, 1.5 Hz, 1H), 5.03 (dt, J = 10.5, 1.5 Hz, 1H), 3.67 (s, 3H), 1.61−1.41 (m, 2H), 1.29−1.14 (m, 6H), 0.83 (t, J = 6.7 Hz, 3H). ^{13}C NMR (75 MHz, $CDCl_3$): δ = 167.2, 165.3, 137.8, 131.4, 131.3, 130.9, 130.8, 129.6, 129.5, 129.4, 115.7, 73.8, 51.2, 34.5, 31.8, 24.9, 22.7, 14.1. MS (EI): m/z = 285 (18), 186 (100). HRMS-(ESIpos): [M + Na]$^+$ calcd for $C_{24}H_{28}O_4SNa$ 435.1600, found 435.1604. IR (neat): 3064, 2931, 2858, 2349, 1984, 1719, 1684, 1629, 1579, 1475, 1442, 1432, 1296, 1278, 1225, 1180, 1120, 1075, 1053, 998, 954, 921, 813, 769, 742, 684, 664. The enantiomeric excess was determined by chiral HPLC using a Chiralpack AS-3 150 × 4.6 mm coloumn. Solvent system: *n*-heptane + 0.1% *i*-PrOH/*i*-PrOH 9/1; flow rate 0.7 mL/min; T = 25 °C.

*Allyl-1-d_2 Methyl 2-(Diphenylsulfuranylidene)malonate (**1k**).* The compound was prepared following the general procedure. Purification by column chromatography over silica (isohexane/ethyl acetate 1/1) afforded the title compound as a colorless oil (93.2 mg, 0.27 mmol, 54%). R_f = 0.2. ^{1}H NMR (400 MHz, $CDCl_3$): δ = 7.65−7.59 (m, 4H), 7.54−7.43 (m, 6H), 5.89 (dd, J = 17.2, 10.5 Hz, 1H), 5.31 (dd, J = 17.2, 1.7 Hz, 1H), 5.14 (dd, J = 10.5, 1.7 Hz, 1H), 3.68 (s, 3H) ppm. ^{13}C NMR (101 MHz, $CDCl_3$): δ = 166.9, 165.8, 133.4, 131.5, 130.6, 129.6, 129.5, 117.1, 77.4, 51.2 ppm. The deuterated C cannot be observed. MS-(EI): m/z = 344 (1), 186 (100), 119 (15). HRMS-(ESIpos): [M + Na]$^+$ calcd for $C_{19}H_{16}D_2O_4SNa$ 367.0943, found 367.0946.

*(E)-Hept-2-en-1-yl Methyl 2-(Diphenylsulfuranylidene)malonate (**1l**).* The compound was prepared following the general procedure. Purification by column chromatography over silica (*n*-pentane/ethyl acetate 1/1) afforded the title compound as a colorless oil (97.1 mg, 0.24 mmol, 49%). R_f = 0.20. ^{1}H NMR (300 MHz, $CDCl_3$): δ = 7.69−7.56 (m, 4H), 7.56−7.40 (m, 6H), 5.78−5.61 (m, 1H), 5.57−5.42 (m, 1H), 4.50 (dd, J = 6.0, 0.9 Hz, 2H), 3.67 (s, 3H), 2.06−1.92 (m, 2H), 1.37−1.18 (m, 4H), 0.87 (t, J = 7.1 Hz, 3H) ppm. ^{13}C NMR (75 MHz, $CDCl_3$): δ = 167.0, 165.9, 134.9, 131.4, 130.8, 129.5, 129.5, 125.1, 64.5, 60.2, 51.2, 32.1, 31.3, 22.3, 14.0 ppm. MS (EI): m/z = 398 (0.2), 186 (100). HRMS (ESIpos): calcd for $C_{23}H_{26}O_4NaS$ 421.1443, found 421.1446. IR (neat): ν = 3061, 2952, 2927, 2871, 2297, 1720, 1685, 1630, 1579, 1475, 1442, 1432, 1377, 1299, 1278, 1225, 1181, 1072, 1024, 999, 971, 915, 824, 769, 744, 685 cm^{-1}.

*Methyl 3-Methylbut-2-en-1-yl 2-(Diphenylsulfuranylidene)-malonate (**1m**).* The compound was prepared following the general procedure. Purification by column chromatography over silica (isohexane/ethyl acetate 1/1) afforded the title compound as a colorless oil (109 mg, 0.29 mmol, 59%). R_f = 0.16. ^{1}H NMR (300 MHz, $CDCl_3$): δ = 7.65−7.57 (m, 4H), 7.52−7.42 (m, 6H), 5.31−5.23 (m, 1H), 4.55 (d, J = 7.0 Hz, 2H), 3.66 (s, 3H), 1.69 (d, J = 0.7 Hz, 3H), 1.63 (s, 3H) ppm. ^{13}C NMR (75 MHz, $CDCl_3$): δ = 167.0, 166.1, 137.2, 131.3, 130.8, 129.5, 129.5, 120.1, 60.7, 60.0, 51.2, 25.8, 18.1 ppm. MS (EI): m/z = 370 (2), 285 (10), 186 (100), 161 (12), 121 (13). HRMS-(ESIpos): [M + Na]$^+$ calcd for $C_{21}H_{22}O_4SNa$ 393.1131, found 393.1134. IR (neat): ν = 3062, 2945, 2243, 1975, 1715, 1682, 1646, 1628, 1579, 1475, 1442, 1432, 1374, 1331, 1301, 1276, 1225, 1121, 1057, 1024, 999, 977, 952, 913, 837, 769, 745, 685 cm^{-1}.

*Methyl Pent-3-en-2-yl 2-(Diphenylsulfuranylidene)malonate (**1n**).* The compound was prepared following the general procedure. Purification by column chromatography over silica (*n*-pentane/ethyl acetate 1/1) afforded the title compound as a colorless oil (156 mg, 0.42 mmol, 84%). R_f = 0.32. ^{1}H NMR (300 MHz, $CDCl_3$): δ = 7.61 (dt, J = 3.8, 2.5 Hz, 4H), 7.54−7.41 (m, 6H), 5.60 (dt, J = 9.3, 6.5 Hz, 1H), 5.39−5.27 (m, 2H), 3.68 (s, 3H), 1.61 (dd, J = 6.5, 0.6 Hz, 3H), 1.15 (d, J = 6.3 Hz, 3H) ppm. ^{13}C NMR (75 MHz, $CDCl_3$): δ = 167.3, 165.2, 131.9, 131.3, 131.0, 129.5, 129.4, 126.8, 70.1, 60.2, 51.2, 20.7, 17.8 ppm. MS (EI): m/z = 285 (13), 186 (100), 161 (16), 121 (14). HRMS-(ESIpos): [M + Na]$^+$ calcd for $C_{21}H_{22}O_4SNa$ 393.1131, found 393.1134. IR (neat): ν = 3061, 2974, 2945, 1717, 1682, 1630, 1579, 1476, 1442, 1432, 1331, 1297, 1227, 1180, 1136, 1062, 1039, 999, 965, 895, 857, 804, 770, 744, 685, 663 cm^{-1}.

*Methyl 3-(Benzyl(but-2-en-1-yl)amino)-2-(diphenylsulfuranylidene)-3-oxopropanoate (**10**).* The compound was prepared following

DOI: 10.1021/acs.joc.5b00666
J. Org. Chem. 2015, 80, 5719−5729

the general procedure. Purification by column chromatography over silica (isohexane/ethyl acetate 2/1) afforded the title compound as a yellow oil (140 mg, 0.34 mmol, 67%). R_f = 0.19. ^{1}H NMR (300 MHz, $CDCl_3$): δ = 7.74−7.65 (m, 4H), 7.53−7.39 (m, 6H), 7.21−7.11 (m, 3H), 6.99 (dd, J = 7.3, 2.0 Hz, 2H), 5.43−5.30 (m, 2H), 4.58 (s, 2H), 3.83 (d, J = 4.4 Hz, 2H), 3.56 (s, 3H), 1.61 (d, J = 4.6 Hz, 3H) ppm. ^{13}C NMR (75 MHz, $CDCl_3$): δ = 168.4, 166.0, 138.6, 131.9, 131.1, 129.9, 129.4, 128.3, 128.2, 127.7, 127.5, 126.6, 59.4, 53.5, 50.5, 17.8 ppm. MS (EI): m/z = 200 (16), 186 (100), 91 (26). HRMS-(ESIpos): $[M + Na]^+$ calcd for $C_{27}H_{27}NO_3SNa$ 468.1603, found 468.1608. IR (neat): ν = 3061, 3026, 2944, 2916, 2854, 2239, 1961, 1739, 1645, 1588, 1574, 1494, 1475, 1441, 1431, 1407, 1359, 1279, 1233, 1179, 1131, 1098, 1075, 1023, 999, 970, 950, 910,728, 686 cm^{-1}.

General Procedure for Cyclopropanation. A solution of sulfonium ylide (0.2 mmol) and Echavaren's catalyst (0.01 mmol) was dissolved in dry toluene. The resulting mixture was heated to 100 °C until TLC showed complete consumption of the ylide. The resulting solution was cooled to room temperature and directly purified by column chromatography affording the desired cyclopropanation product.

*Methyl 2-Oxo-4-pentyl-3-oxabicyclo[3.1.0]hexane-1-carboxylate (**4j**).* The compound was prepared according to the general procedure using ylide **1j**. Purification by column chromatography over silica (*n*-pentane/ethyl acetate 9/1 to 1/1) afforded the title compound as a colorless oil (45 mg, 199 μmol, 99%, dr = 95:5). R_f = 0.68 (*n*-pentane/ethyl acetate 1/1). ^{1}H NMR (300 MHz, $CDCl_3$): δ = 4.28 (t, J = 6.2 Hz, 1H), 3.80 (s, 3H), 2.50 (dd, J = 8.1, 5.5 Hz, 1H), 2.02 (dd, J = 8.1, 4.7 Hz, 1H), 1.74−1.62 (m, 1H), 1.48−1.23 (m, 8H), 0.87 (t, J = 6.9 Hz, 3H) ppm. ^{13}C NMR (75 MHz, $CDCl_3$): δ = 170.2, 167.5, 79.0, 53.0, 36.0, 32.7, 31.5, 29.8, 23.8, 22.5, 21.1, 14.0. MS (EI): m/z = 155 (100), 127 (23), 95 (12) ppm. HRMS (ESIpos): calcd for $C_{12}H_{18}O_4Na$: 249.1097, found 249.1096. IR (neat): ν (cm^{-1}) = 2955, 2932, 2860, 2318, 1776, 1728, 1439, 1377, 1349, 1308, 1264, 1231, 1202, 1174, 1125, 1095, 1083, 1045, 991, 945, 912, 790, 771, 729 cm^{-1}. The enantiomeric excess was determined by chiral GC using a IVADEX 1/PS 086 G 548 (25 m) column: temp 80 1N 180 10/MIN 220; 0.4 bar H_2. Minor enantiomer t_R = 72.28 min.Major enantiomer: t_R = 73.32 min.

*Methyl 4-Butyl-2-oxo-3-oxabicyclo[3.1.0]hexane-1-carboxylate (**4l**).* The compound was prepared according to the general procedure using ylide **1l**. Purification by column chromatography over silica (*n*-pentane/ethyl acetate 5/1 to 1/1) afforded the title compound as a colorless oil (27 mg, 0.13 mmol, 82%, dr = 95:5). R_f = 0.68 (*n*-pentane/ethyl acetate 1/1). ^{1}H NMR (300 MHz, $CDCl_3$): δ 4.29 (t, J = 6.2 Hz, 1H), 3.82 (s, 3H), 2.54−2.45 (m, 1H), 2.04 (dd, J = 8.1, 4.7 Hz, 1H), 1.71 (ddd, J = 13.2, 7.9, 4.9 Hz, 2H), 1.49−1.22 (m, 5H), 0.92 (t, J = 7.0 Hz, 3H) ppm. ^{13}C NMR (75 MHz, $CDCl_3$): δ 170.2, 167.6, 79.1, 53.1, 35.8, 32.7, 29.9, 26.3, 22.5, 21.2, 14.0 ppm. MS (EI): m/z = 155 (100), 127 (32), 123 (10), 95 (17), 59 (10). HRMS (ESIpos): calcd for $C_{11}H_{16}O_4Na$ 212.24, found 212.24. IR (neat): ν (cm^{-1}) = 2956, 2933, 2862, 1777, 1728, 1439, 1376, 1349, 1309, 1265, 1202, 1174, 1094, 1047, 979, 937, 911, 788, 767, 734 cm^{-1}.

*Methyl 3-Benzyl-6-methyl-2-oxo-3-azabicyclo[3.1.0]hexane-1-carboxylate (**11**).* The compound was prepared according to the general procedure using ylide **10**. Purification by column chromatography over silica (isohexane/ethyl acetate 2/1 to 1/1) afforded the title compound as a colorless oil (45 mg, 199 μmol, 99%, dr = 4.5:1). R_f = 0.34 (isohexane/ethyl acetate 1/1). ^{1}H NMR (300 MHz, $CDCl_3$): δ = 7.31−7.07 (m, 5H), 4.43 (d, J = 14.6 Hz) and 4.39 (d, J = 14.6 Hz) (1H), 4.18 (d, J = 14.6 Hz) and 4.16 (d, J = 14.6 Hz) (1H), 3.75 (s) and 3.72 (s) (1H), 3.38 (dd, J = 11.0, 6.4 Hz) and 3.32 (dd, J = 10.2, 5.8 Hz) (1H), 3.02 (d, J = 10.2 Hz) and 2.90 (d, J = 11.0 Hz) (1H), 2.27−2.15 (m) and 2.05 (t, J = 5.4 Hz, 1H), 1.39−1.27 (m, 1H), 1.19 (d, J = 6.1 Hz) and 0.88 (d, J = 6.4 Hz) (1H) ppm. ^{13}C NMR (75 MHz, $CDCl_3$): δ = 170.2, 169.7, 168.0, 167.3, 136.5, 136.0, 128.8, 128.8, 128.3, 127.9, 127.8, 52.6, 52.5, 46.7, 46.6, 43.1, 37.2, 36.9, 29.6, 27.7, 26.6, 25.6, 12.2, 7.1 ppm. MS (EI): m/z = 259 (64), 227 (67), 199 (60), 118 (30), 109 (12), 95 (19), 91 (100), 65 (20). HRMS (ESIpos): calcd for $C_{15}H_{17}O_3NNa$ 282.1106, found 282.1099.

■ ASSOCIATED CONTENT

Ⓢ Supporting Information

Crystallographic data, details of mechanistic experiments, documentation of theoretical calculations, NMR spectra, and chromatograms. The Supporting Information is available free of charge on the ACS Publications website at DOI: 10.1021/acs.joc.5b00666.

■ AUTHOR INFORMATION

Corresponding Authors

*E-mail: veiros@ist.utl.pt.

*E-mail: nuno.maulide@univie.ac.at.

Notes

The authors declare no competing financial interest.

■ ACKNOWLEDGMENTS

Generous support of this research by the Deutsche Forschungsgemeinschaft (DFG, Grants MA 4861/4-1 and/4-2) and the University of Vienna is acknowledged. Mrs. U. Rosentreter (MPI Mülheim) and Mrs. E. Macoratti (U. Vienna) are acknowledged for analytical determination. Parts of this research were carried out at the Max-Planck-Institut für Kohlenforschung, which we gratefully acknowledge. L.F.V. acknowledges Fundação para a Ciência e Tecnologia, Projecto Estratégico - PEst-OE/QUI/UI0100/2013.

■ REFERENCES

(1) For selected reviews on gold(I) catalysis, see: (a) Dyker, G. *Angew. Chem., Int. Ed.* **2000**, *39*, 4237. (b) Hoffmann-Röder, A.; Krause, N. *Org. Biomol. Chem.* **2005**, *3*, 387. (c) Hashmi, A. S. K.; Hutchings, G. *Angew. Chem., Int. Ed.* **2006**, *45*, 7896. (d) Fürstner, A.; Davies, P. W. *Angew. Chem., Int. Ed.* **2007**, *46*, 3410. (e) Jimenez-Nunez, E.; Echavarren, A. M. *Chem. Commun.* **2007**, 333. (f) Hashmi, A. S. K. *Chem. Rev.* **2007**, *107*, 3180. (g) Li, Z.; Brouwer, C.; He, C. *Chem. Rev.* **2008**, *108*, 3239. (h) Arcadi, A. *Chem. Rev.* **2008**, *108*, 3266. (i) Shen, H. C. *Tetrahedron* **2008**, *64*, 3885. (j) Shen, H. C. *Tetrahedron* **2008**, *64*, 7847. (k) Fürstner, A. *Chem. Soc. Rev.* **2009**, *38*, 3208. (l) Shapiro, N.; Toste, F. D. *Synlett* **2010**, 675. (m) Bandini, M. *Chem. Soc. Rev.* **2011**, *40*, 1358.

(2) (a) Chiarucci, M.; Bandini, M. *Beilstein J. Org. Chem.* **2013**, *9*, 2586. (b) Marion, N.; Nolan, S. P. *Chem. Soc. Rev.* **2008**, *37*, 1776.

(3) For selected examples, see: (a) Yang, C.; He, C.-G. *J. Am. Chem. Soc.* **2005**, *127*, 6966. (b) LaLonde, R. L.; Brenzovich, W. E., Jr.; Benitez, D.; Tkatchouk, E.; Kelley, K.; Goddard, W. A., III; Toste, F. D. *Chem. Sci.* **2010**, *1*, 226. (c) Brouwer, C.; He, C. *Angew. Chem., Int. Ed.* **2006**, *45*, 1744. (d) Bender, C.-F.; Widenhoefer, R. A. *Chem. Commun.* **2006**, 4143. (e) Han, X.; Widenhoefer, R. A. *Angew. Chem., Int. Ed.* **2006**, *45*, 1747. (f) Liu, X.-Y.; Li, C. H.; Che, C. M. *Org. Lett.* **2006**, *8*, 2707. (g) Li, H.; Song, F.; Widenhoefer, R. A. *Adv. Synth. Catal.* **2011**, *353*, 955. (h) Kanno, O.; Kuriyama, W.; Wang, Z. J.; Toste, F. D. *Angew. Chem., Int. Ed.* **2011**, *50*, 9919.

(4) For examples, see: (a) Zhou, C.-Y.; Che, C.-M. *J. Am. Chem. Soc.* **2007**, *129*, 5828. (b) Wang, M.-Z.; Wong, M.-K.; Che, C.-M. *Chem.—Eur. J.* **2008**, *14*, 8353. (c) Xiao, Y.-P.; Liu, X.-Y.; Che, C.-M. *Angew. Chem., Int. Ed.* **2011**, *50*, 4937. (d) Xiao, Y.-P.; Liu, X.-Y.; Che, C.-M. *Beilstein J. Org. Chem.* **2011**, *7*, 1100. (e) Rao, W.; Susanti, D.; Chan, P. W. H. *J. Am. Chem. Soc.* **2011**, *133*, 15248. (f) Huang, X.; Klimczyk, S.; Veiros, L. F.; Maulide, N. *Chem. Sci.* **2013**, *4*, 1105.

(5) Huang, X.; Peng, B.; Luparia, M.; Gomes, L.; Veiros, L. F.; Maulide, N. *Angew. Chem., Int. Ed.* **2012**, *51*, 8886.

(6) (a) Nieto-Oberhuber, C.; López, S.; Muñoz, M. P.; Cárdenas, D. J.; Buñuel, E.; Nevado, C.; Echavarren, A. M. *Angew. Chem., Int. Ed.* **2005**, *44*, 6146. (b) Pérez-Galán, P.; Delpont, N.; Herrero-Gómez, E.; Maseras, F.; Echavarren, A. M. *Chem.—Eur. J.* **2010**, *16*, 5234. (c) López-Carrillo, V.; Echavarren, A. M. *J. Am. Chem. Soc.* **2010**, *132*,

DOI: 10.1021/acs.joc.5b00666
J. Org. Chem. 2015, 80, 5719−5729

9292. (d) Homs, A.; Obradors, C.; Leboeuf, D.; Echavarren, A. M. *Adv. Synth. Catal.* **2014**, *356*, 1.

(7) The ^{31}P NMR shift for the free ligand 6 is δ = 21.4 ppm; for comparison, see: (a) Huang, X.; Anderson, K. W.; Zim, D.; Jiang, L.; Klapars, A.; Buchwald, S. L. *J. Am. Chem. Soc.* **2003**, *125*, 6653. The ^{31}P NMR shift for the phosphine oxide of ligand **6** is δ = 53.7 ppm; for comparison, see: (b) Zhang, D.; Gua, A.; Doan, C.; Stewart, T.; Bau, R.; Selke, M. *Org. Lett.* **2010**, *10*, 3100.

(8) Parr, R. G.; Yang, W. In *Density Functional Theory of Atoms and Molecules*; Oxford University Press: New York, 1989.

(9) The single-point free energy values presented here and in ref 4f result from different solvation models. In ref 4f, it was used the PCM model as implemented in Gaussian 03 with a molecular cavity based on the united atom topological model applied on UAHF radii, optimized for the HF/6-31G(d). Here, we used the PCM model as implemented in Gaussian 09 with with radii and nonelectrostatic terms of the SMD solvation model, developed by Truhler et al. (see the Computational Details in the Supporting Information).

(10) (a) Wiberg, K. B. *Tetrahedron* **1968**, *24*, 1083. (b) Wiberg indices are electronic parameters related to the electron density between atoms. They can be obtained from a natural population analysis and provide an indication of the bond strength..

(11) For examples of metal−cyclopropane σ-complexes, see: (a) Youngs, W. J.; Simms, B. L.; Ibers, J. A. *J. Organomet. Chem.* **1994**, *272*, 295. (b) Youngs, W. J.; Ibers, J. A. *Organometallics* **1983**, *2*, 979. (c) Cutler, A.; Fish, R. W.; Giering, W.; Rosenblum, M. *J. Am. Chem. Soc.* **1972**, *94*, 4354.

(12) For literature precedents on SN_2-type displacement at tertiary sp^3-carbon electrophiles, see: (a) Pronin, S. V.; Reiher, C. A.; Shenvi, R. A. *Nature* **2013**, *501*, 195. (b) Mascal, M.; Hafezi, N.; Toney, M. D. *J. Am. Chem. Soc.* **2010**, *132*, 10662.

(13) See the Supporting Information for further details.

(14) For a similar rearrangement, see: (a) Marion, N.; Gealageas, R.; Nolan, S. P. *Org. Lett.* **2007**, *9*, 2653. For a computational study of related processes, see: (b) Paton, R. S.; Maseras, F. *Org. Lett.* **2009**, *11*, 2237.

(15) For the reverse of this hypothetical reaction, the Overman rearrangement, see: (a) Overman, L. E. *J. Am. Chem. Soc.* **1976**, *98*, 2901. (b) Anderson, C. E.; Overman, L. E. *J. Am. Chem. Soc.* **2003**, *125*, 92697. For a gold-catalyzed version, see: (c) Xing, D.; Yang, D. *Beilstein J. Org. Chem.* **2011**, *7*, 781.

(16) For our previously reported ylide transfer, see: Huang, X.; Goddard, R.; Maulide, N. *Angew. Chem., Int. Ed.* **2010**, *49*, 8979.

DOI: 10.1021/acs.joc.5b00666
J. Org. Chem. 2015, 80, 5719−5729